Oxygen atom Rydberg time-of-flight spectroscopy

Cheng Lin, Mark F. Witinski, and H. Floyd Davis[a)]
Department of Chemistry and Chemical Biology, Baker Laboratory, Cornell University, Ithaca, New York 14853

(Received 2 December 2002; accepted 1 April 2003)

The Rydberg atom time-of-flight method has been employed for velocity, angular and spin–orbit state-resolved detection of oxygen atoms, O (^3P_J). The atoms were ''tagged'' by double-resonance two-photon excitation to high-n Rydberg levels and subsequently field ionized at a detector. The method was characterized by studying a well-known system, the photodissociation of NO_2 at 355 nm. From the O atom time-of-flight spectra, the NO vibrational distribution for different O (^3P_J) levels was obtained, with NO ($v=1$) rotational structure partially resolved. © *2003 American Institute of Physics.* [DOI: 10.1063/1.1576752]

I. INTRODUCTION

Atoms in states of high principal quantum number (Rydberg atoms) possess unique properties such as long lifetimes and susceptibility to field ionization.[1] The H-atom Rydberg time-of-flight (HRTOF) method has been widely employed in studies of photodissociation and bimolecular reaction dynamics yielding H and D atom products. In HRTOF, H or D atoms are photoexcited to high-n levels immediately after being produced, and allowed to fly as neutrals to a detector where they are field ionized and counted.[2] The primary advantages of this method are: (1) products evolve spatially as neutrals, thus avoiding resolution-limiting space-charge effects; (2) products are selected spectroscopically, so mass analysis is not necessary; (3) the relative uncertainty in flight length ($\Delta l/l$) can be made much smaller than is possible with conventional photofragment spectroscopy using electron impact ionization; and (4) because photoexcitation is doubly resonant, high efficiencies may be achieved during the Rydberg tagging process.

A 1996 review by Ashfold summarizes the use of HRTOF for studying the photodissociation of a number of prototypical small polyatomic molecules.[3] More recently, the list of species studied using this method has grown to include free radicals such as C_2H_3,[4] C_2H_5,[5] and H_2CN.[6] Because H or D atom fragments are much lighter than their counterfragments, measured recoil velocities are far larger than the initial velocity of the parent molecule, leading to very small uncertainties in measured kinetic energy release distributions. As a result, vibrational resolution is routinely achieved, and in favorable cases, rotational structure can be observed. HRTOF has also been employed in studies of bimolecular reaction dynamics and inelastic collisions. Using this technique, rovibrational quantum state-resolved differential cross sections were obtained for the $H+D_2$ isotope exchange reaction by Welge's group[7] and for the O (^1D)$+H_2 \rightarrow OH+H$ reaction by Yang and co-workers.[8] We have employed this method to observe mode-specific energy disposal in the four-atom reaction $OH+D_2 \rightarrow HOD+D$,[9] and have also studied the inelastic scattering of Rydberg H and D atoms from N_2 and O_2 in crossed molecular beams.[10]

In time-of-flight measurements, the experimental uncertainty in the measured velocity of a fragment X recoiling from counterfragment R is primarily associated with the uncertainty in the distance through which the particle travels to the detector. For a given experimental uncertainty in measured velocity (dv_x), the uncertainty in the derived relative translational energy (dE) increases with increasing mass of particle X as

$$\frac{dE}{dv_x} = \sqrt{2Em_x\left(1+\frac{m_x}{m_R}\right)},$$

where m_x and m_R denote the mass of the detected fragment and counterfragment, respectively. Clearly, detection of H or D atoms provides the greatest possible energy resolution. However, even for an atom such as oxygen recoiling from a small molecule, the resolution can still be sufficient to resolve the product internal state distribution of the counterfragment. Furthermore, individual spin–orbit states of O (^3P_J) can be selected in the Rydberg tagging process, making it possible to study the correlation between atomic photofragment spin–orbit state and the internal state distribution of the molecular counterfragment in photodissociation or bimolecular reaction dynamics.

Velocity-resolved studies employing Rydberg tagging have primarily focused on H and D atoms, in part because flight times are typically < 30 μs (assuming a 30 cm flight distance), which are considerably shorter than Rydberg lifetimes in the absence of external electric fields. This guarantees that the experimental sensitivity is not preferentially biased towards the fastest species surviving as Rydberg atoms before reaching the detector. For detection of heavier atoms and molecules, which are typically produced with substantially smaller velocities, the question of whether Rydberg lifetimes exceed flight times becomes a critical issue in establishing the feasibility of Rydberg tagging as a detection method. Zare and co-workers have shown that the highest Rydberg states of HD ($n>100$) have lifetimes of at least 20 μs.[11] Rydberg states of NO have also been shown to have

a)Electronic mail: hfd1@cornell.edu

long lifetimes;[12] this feature has been utilized by Softley's group in Rydberg tagging detection of NO.[13] Mueller *et al.* have used Rydberg tagging to detect both the O and NO products from NO_2 photodissociation.[14] In all of the aforementioned experiments, although it was clear that a fraction of the initially prepared Rydberg states survived their transit time to the field ionization detector (typically over a time of tens of microseconds), the actual Rydberg lifetimes were not determined.

The lifetimes of Rydberg levels of atoms and molecules have received considerable experimental and theoretical attention. It is now quite well established that the presence of electric fields, either stray fields or fields due to ionic byproducts produced by the lasers, can lead to significant enhancements in Rydberg lifetimes over the expected n^3 behavior.[15] Indeed, Schlag's group has shown that the intentional inclusion of a small electric field during the Rydberg excitation process can significantly enhance the lifetimes of Rydberg states in ZEKE spectroscopy experiments.[16,17]

Direct experimental measurements of Rydberg lifetimes are complicated significantly by bulk transport of the sample during the several hundred microsecond time scale of the measurement. Although this difficulty has been elegantly surmounted in recent experiments through the use of cold atom trapping techniques,[18] this method of measuring Rydberg lifetimes is not well suited to atoms such as oxygen. In order to assess its viability as a general detection method in future crossed molecular beams reactive scattering studies, we have characterized the technique of oxygen Rydberg time-of-flight spectroscopy (ORTOF). Photodissociation of NO_2 at 355 nm producing NO($^2\Pi_\Omega$, $v=0,1$; J) and O ($^3P_J, J=0,1,2$) was chosen as the source of O atoms because there exists an abundance of literature on this system, allowing for a comparison of our experimental results with those from other studies.

II. EXPERIMENT

The experiments were carried out using a fixed source, rotatable detector crossed molecular beams apparatus.[9,10] A mixture of NO_2 in argon carrier gas (backing pressure ~5 psig) was expanded from a piezoelectric pulsed valve. In order to reduce the interference from clustering, the NO_2 concentration was kept low (0.25%) by placing the sample in a low temperature bath (chlorobenzene slush). The NO_2 beam passed through a skimmer into a separately pumped chamber where it was intersected by the photolysis and probe lasers. The photolysis laser (355 nm) was a Continuum Powerlite 9030 Nd:YAG laser. The polarization of the photolysis laser could not be rotated in the plane of the molecular beam and the detector due to a geometrical constraint. However, information about the photofragment anisotropy could be obtained by taking TOF spectra at a range of different laboratory detection angles. Figure 1 shows the doubly resonant two-photon excitation scheme used to promote the oxygen atom products to high-n Rydberg levels.[19] The first photon was tuned to the $^3S_1 \leftarrow {}^3P_J$ transition (~130 nm) of oxygen, while the second photon (~306 nm) excited atoms

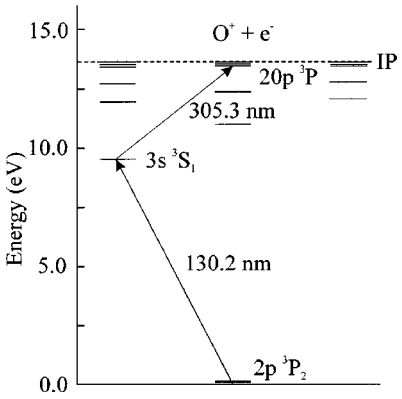

FIG. 1. Two-photon excitation scheme for production of Rydberg oxygen atoms.

from the $^3S_1$ state to a Rydberg level. No special shielding was used to protect the interaction region from stray electric or magnetic fields.

Pulsed 130 nm radiation was produced by resonance enhanced four-wave mixing ($\omega_{VUV}=2\omega_R-\omega_T$) in a krypton gas cell.[20] The wave number of the frequency-doubled dye laser (ω_R) was fixed to the two-photon resonance transition to the $5p[1/2]_0$ level of Kr, and that of the other dye laser (ω_T) was varied to produce tunable radiation around 130 nm. The two laser beams were combined using a dielectric mirror and focused by an achromatic lens into the gas cell through a quartz entrance window. The VUV light then passed through a MgF_2 window into the interaction region. Excitation to high-n Rydberg levels was accomplished using the doubled output of a third dye laser, which we denote as the Rydberg laser. All three dye lasers (Lambda Physik Scanmate 2) were pumped by another Continuum Powerlite 9030 Nd:YAG laser, and the optical paths were carefully adjusted to achieve the crucial temporal overlap for four-wave mixing. The "tagged" O atoms then flew 29.2 cm through a field-free region before passing through a wire mesh grid typically held at +30 V to reject positive ions, followed by a second grounded wire mesh grid. The two grids were located 1.4 and 1.0 cm away from the surface of the microchannel plate (MCP), respectively. The Rydberg atoms were field ionized (2000 V/cm) in the region between the grounded mesh and the MCP, and then collected on the MCP. The ion signal was amplified by an EG&G VT120 preamplifier, and the time-of-flight (TOF) spectra were recorded by an SR430 multichannel scaler.

Because the Rydberg excitation laser (306 nm) is also capable of dissociating NO_2, a separate set of scans was run with the 355 nm laser blocked, and this signal was subtracted from the total.

III. RESULTS AND DISCUSSION

Figure 2 shows the Rydberg excitation spectrum recorded by scanning the Rydberg tagging dye laser while holding the photolysis and VUV lasers at fixed wavelengths. The progression of peaks corresponds to excitation to Rydberg levels ranging from $n=14$ to $n=48$. The signal intensity of each peak depends on several factors, such as the oscilla-

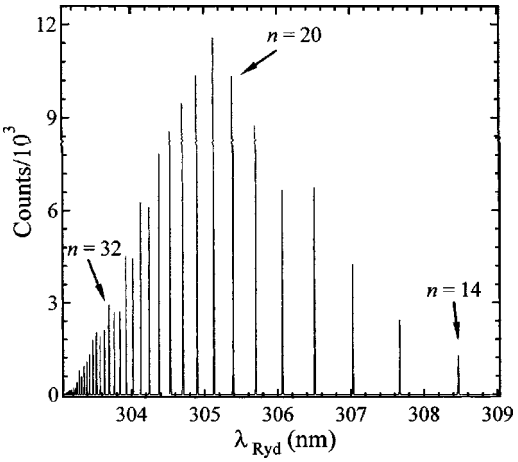

FIG. 2. Rydberg excitation spectrum obtained by scanning the Rydberg tagging laser and monitoring the integrated O Rydberg atom intensity at $\theta=20°$.

tor strength for the excitation process, the fraction of Rydberg atoms surviving to the detector, and the fraction of Rydberg atoms field ionized at the detector. It was found that excitation to $n=21$ produced the largest signal level.

For ORTOF to be useful as a general detection method, it is desirable that O atom detection efficiency be independent of its velocity. Of particular concern is the possibility that detection sensitivity is biased towards faster products due to their lower probability of loss en route to the detector. Loss mechanisms include radiative decay and ionization processes. In order to examine how the velocity and n level of a Rydberg oxygen atom affect its probability of being detected, we have acquired TOFs for a range of Rydberg n levels at the same laboratory angle, as shown in Fig. 3. The two prominent peaks in the TOF spectrum correspond to O atoms that have recoiled from NO in $v=0$ (shorter time) and $v=1$ (longer time). It is clear from the figure that the relative intensities of the two main features are not exactly the same for all Rydberg levels. In Fig. 3, the intensities of the faster peak in each spectrum have been scaled to be equal to one another. For $n=14$, the lowest Rydberg level studied, the

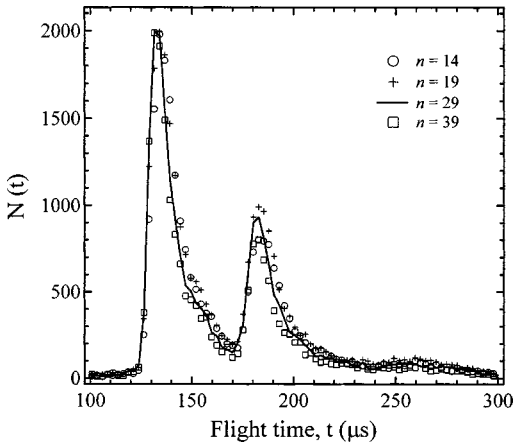

FIG. 3. TOF spectra for O (^3P_J) from 355 nm photolysis of NO_2 recorded at $\theta=30°$. Spectra for $n=14$, 29, and 39 have each been normalized to make the intensities of the faster peak equal to one another.

intensity of the slower peak is smaller than that for $n=19$. The preferential loss of the slower atoms most likely results from the fact that the radiative decay lifetime of high-n Rydberg atoms scales as n^3-n^5 depending on the extent of l and m_l state mixing.[15] On the other hand, the $v=1$ weight also decreased as the Rydberg excitation laser wavelength was tuned to excite O atoms to the highest n level studied, $n=39$. Because these atoms are very close to the ionization threshold, ionization of very high-n Rydbergs by stray fields before reaching the detector is more likely to occur, accounting for the preferential loss of the slower moving Rydberg atoms. Due to the presence of a positive voltage on the first wire mesh, any Rydberg atoms that become ionized during their transit to the detector cannot reach the microchannel plate and are not detected.

A noticeable effect in Fig. 3 is that the slow edge of each TOF spectrum is shifted to longer times for successively lower-n Rydberg levels. This effect results from the fact that for a given electric field, the rate of ionization of Rydberg atoms in low-n levels is smaller than for atoms in higher-n levels. Because of the reduced rate of field ionization, Rydberg atoms in lower-n levels are on average able to penetrate further past the final wire mesh into the high-field region prior to ionization, resulting in a slightly longer effective neutral flight path. In the near future, we plan to reconfigure the detector by moving the wire meshes substantially closer to the MCP, thereby increasing the electric field strength and decreasing the uncertainty in the neutral flight path. This should reduce this type of broadening of the TOF spectrum. The relative contributions to the TOF spectra from $v=0$ and $v=1$ are essentially the same for $n=19$–29. Since the radiative decay lifetimes should exhibit an n^3-n^5 dependence, the Rydberg lifetimes in this range of n must be long compared to the flight time ($\sim$200 μs) under our experimental conditions. Thus, we believe that after making the change in detector geometry noted above, the ''optimum'' n level for ORTOF studies will lie in the range $n=19$–29.

The top panel of Fig. 4 shows an experimental TOF for O ($^3P_2$) channel at a laboratory angle of 30°, together with a fit (solid line) generated using a forward convolution program. The program took as input a translational energy distribution, $P(E)$, for each of the two NO vibrational energy levels ($v=0$ and 1), as well as their respective relative weights and anisotropy parameters (β). The program averaged over the known experimental parameters such as the beam spatial width and beam velocity spread. The input parameters were iteratively improved until the calculated TOF spectra and angular distributions agreed with the experimental data. In the bottom panel, several late-arriving TOF peaks have been enlarged. These peaks represent O atoms that were produced coincidently with NO ($v=1$) in high rotational states. This ''bimodal'' rotational distribution of NO ($v=1$) produced in the photodissociation of NO_2 has been observed previously, both by Liu and co-workers,[21] and by Reisler *et al.*[22] In fitting the data, we used a third translational energy distribution for this high rotational contribution to NO ($v=1$). In Fig. 5, the optimum $P(E)$s for fitting the $J=2$ data are shown, with the 8% NO ($v=1$, high-J) contribution plotted separately from the rest. For the $^3P_0$ channel, the low

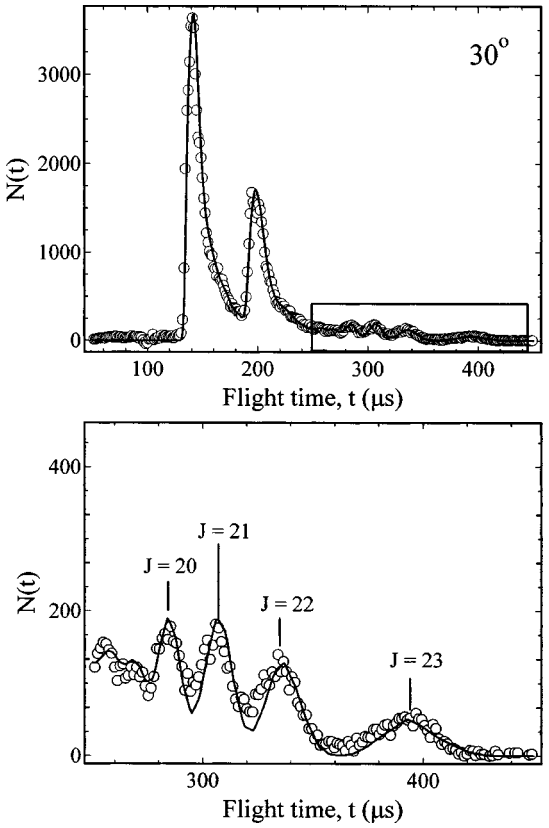

FIG. 4. Top panel: TOF spectrum for O ($^3P_2$) at 30° (open circles) along with fit (solid line). Bottom panel: Expanded region showing rotationally resolved levels of recoiling NO ($v=1$) counterfragment.

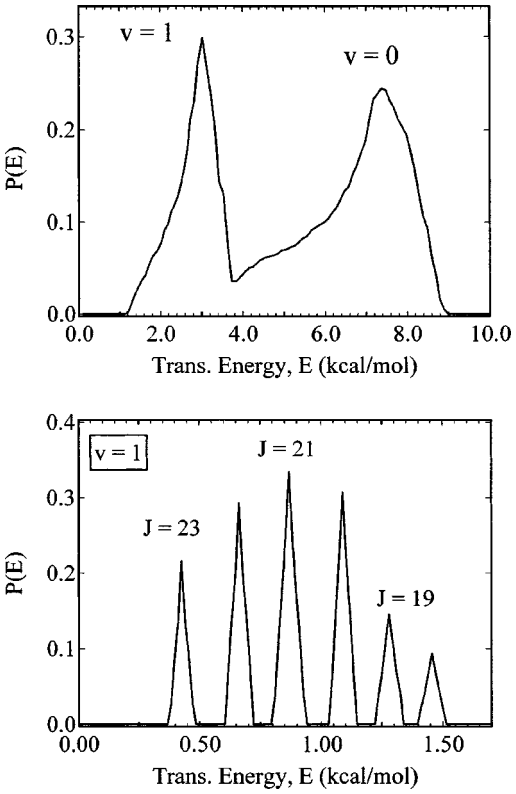

FIG. 5. Translational energy distributions for photodissociation of NO_2 at 355 nm. Top: $v=0$, $v=1$ (low-J). Bottom: $v=1$ (high-J).

signal to noise ratio rendered the fit of the high-J levels of $v=1$ NO impractical, hence only 2 $P(E)$s were used. From the known photon energy and thermochemistry, we have assigned the NO J levels using the optimized $P(E)$s.

From the best fit of the O ($^3P_2$) TOF spectra at all angles, it was found that $62\pm1\%$ of the NO was formed in $v=0$, with the remaining $38\pm1\%$ produced in $v=1$. Reid, Reisler and co-workers[23,24] measured the relative yield of NO ($v=1$) at a wide range of excitation wavelengths, including 355 nm, and compared their experimental values to calculated distributions obtained from variational RRKM theory.[25] Their experimental value of $41.2\pm6.2\%$ was in close agreement with the theoretical value, which at this energy was 39%. The result obtained from our experimental measurement is in good agreement with both of these values. This supports our conclusion that O-atom Rydberg lifetimes under our experimental conditions are long compared to their flight times to the detector. We conclude, therefore, that our ORTOF measurements are not biased in favor of faster species due to Rydberg lifetime issues.

One of the key advantages of this technique is its ability to probe each of the three O (^3P_J) spin–orbit states by simply changing the VUV wavelength (by changing ω_T). By combining spectroscopic detection with TOF measurements, the correlation between O atom J level and the NO internal state distribution can be obtained. We have acquired TOF spectra for each oxygen spin–orbit state over the full range of permissible angles. In Fig. 6 we show TOFs for all three

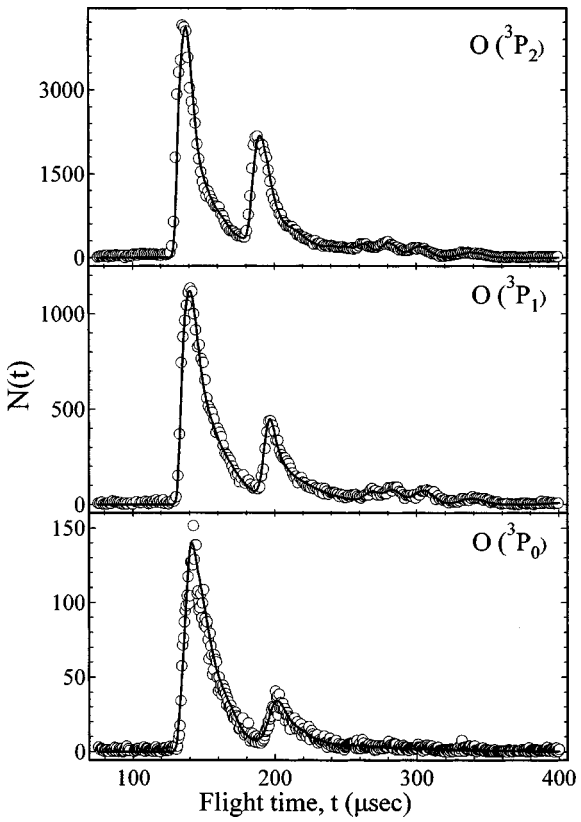

FIG. 6. TOF spectra for O (^3P_J; J=2,1,0) at $\theta = 20°$.

TABLE I. Anisotropy parameters (β) and NO product vibrational energy distributions for the three oxygen spin–orbit levels produced from NO_2 photodissociation at 355 nm.

	$^3P_2$	$^3P_1$	$^3P_0$
β ($v=0$)	1.4±0.1	1.4±0.1	1.3±0.1
β ($v=1$, low-J levels)	1.4±0.1	1.3±0.1	1.3±0.1
β ($v=1$, high-J levels)	0.9±0.2	0.7±0.2	⋯
% ($v=0$)	62±1	70±2	78±2
% ($v=1$, low-J levels)	30±1	23±2	22±2
% ($v=1$, high-J levels)	8±1	8±1	⋯

spin–orbit states of the O atom at the same laboratory angle, 20°. The fits for each state were obtained using the optimized branching ratios and β parameters summarized in Table I. In agreement with the work of both Liu[21] and Reisler,[22] we find that ground-state O ($^3P_2$) is correlated to NO products having the greatest average degree of vibrational excitation, whereas O ($^3P_0$), on average, is correlated to vibrationally colder NO products. From Table I it is also clear that β decreases with internal energy of the recoiling NO fragments. That is, for a given oxygen level, β ($v=0$)$\geqslant\beta$ ($v=1$, low-J)$>\beta$ ($v=1$, high-J). This relationship between anisotropy parameter and internal energy is consistent with the extensive work by the Reisler group, who have explained the trend elegantly using a classical model for nonaxial fragment recoil.[22]

In conclusion, our measurements of the photodissociation of NO_2 at 355 nm are in good agreement with those obtained previously using other experimental means. For the channel leading to production of NO ($v=1$) in high-J levels, rotational resolution was achieved. These studies indicate that ORTOF is suitable as a general method for probing the O (^3P_J) products from photodissociation or bimolecular reactions in crossed molecular beams. In particular, the technique seems well suited for studies of the reaction $H+O_2 \rightarrow OH(2\Pi)+O(^3P_J)$, in which the OH fragment is preferentially formed in high-N levels at collision energies above the reaction endoergicity.[26]

ACKNOWLEDGMENT

This research was supported by the U.S. Department of Energy and by the Alfred P. Sloan Foundation.

[1] F. Gallagher, *Rydberg Atoms* (Cambridge University Press, New York, 1994).
[2] L. Schnieder, W. Meier, K. H. Welge, M. N. R. Ashfold, and C. M. Western, J. Chem. Phys. **92**, 7027 (1990).
[3] M. N. R. Ashfold, D. H. Mordaunt, and S. H. S. Wilson, Adv. Photchem. **21** 217 (1996).
[4] K. Xu and J. Zhang, J. Chem. Phys. **111**, 3783 (1999).
[5] G. Amaral, K. Xu, and J. Zhang, J. Chem. Phys. **114**, 5164 (2001).
[6] E. J. Bernard, B. R. Strazisar, and H. F. Davis, Chem. Phys. Lett. **313**, 461 (1999).
[7] L. Schnieder, K. Seekamp-Rahn, E. Wrede, and K. H. Welge, J. Chem. Phys. **107**, 6175 (1997).
[8] X. Liu, J. J. Lin, S. Harich, G. C. Schatz, and X. Yang, Science **289**, 1536 (2000).
[9] B. R. Strazisar, C. Lin, and H. F. Davis, Science **290**, 958 (2000).
[10] B. R. Strazisar, C. Lin, and H. F. Davis, Phys. Rev. Lett. **86**, 3997 (2001).
[11] F. Merkt, H. Xu, and R. N. Zare, J. Chem. Phys. **104**, 950 (1996).
[12] S. T. Pratt, J. Chem. Phys. **108**, 7131 (1998).
[13] O. L. A. Monti, H. Dickinson, S. R. Mackenzie, and T. P. Softley, J. Chem. Phys. **112**, 3699 (2000).
[14] J. A. Mueller, S. A. Rogers, and P. L. Houston, J. Phys. Chem. A **102**, 9666 (1998).
[15] W. A. Chupka, J. Chem. Phys. **98**, 4520 (1993).
[16] L. Y. Baranov, A. Held, H. L. Selzle, and E. W. Schlag, Chem. Phys. Lett. **291**, 311 (1998).
[17] A. Held, L. Y. Baranov, H. L. Selzle, and E. W. Schlag, Chem. Phys. Lett. **291**, 318 (1998).
[18] Aa. L. de Oliveira, M. W. Mancini, V. S. Bagnato, and L. G. Marcassa, Phys. Rev. A **65**, 031401 (2002).
[19] C. Moore, *Tables of Spectra of Hydrogen, Carbon, Nitrogen, and Oxygen Atoms and Ions* (CRC, Boca Raton, FL, 1993).
[20] J. P. Marangos, N. Shen, H. Ma, M. H. R. Hutchinson, and J. P. Connerade, J. Opt. Soc. Am. B **7**, 1254 (1990).
[21] C.-H. Hsieh, Y.-S. Lee, A. Fujii, S.-H. Lee, and K. Liu, Chem. Phys. Lett. **277**, 33 (1997).
[22] A. V. Demyanenko, V. Dribinski, H. Reisler, H. Meyer, and C. X. W. Qian, J. Chem. Phys. **111**, 7383 (1999).
[23] S. A. Reid and H. Reisler, J. Phys. Chem. **100**, 474 (1996).
[24] M. Hunter, S. A. Reid, D. C. Robie, and H. Reisler, J. Chem. Phys. **99**, 1093 (1993).
[25] S. J. Klippenstein and T. Radivoyevitch, J. Chem. Phys. **99**, 3644 (1993).
[26] M. J. Bronikowski, R. Zhang, D. J. Rakestraw, and R. N. Zare, Chem. Phys. Lett. **156**, 7 (1989).